Defects in purine nucleotide metabolism lead to substantial incorporation of xanthine and hypoxanthine into DNA and RNA

Bo Pang[a,1], Jose L. McFaline[a], Nicholas E. Burgis[b,2], Min Dong[a,3], Koli Taghizadeh[c], Matthew R. Sullivan[a], C. Eric Elmquist[a,4], Richard P. Cunningham[b], and Peter C. Dedon[a,c,5]

[a]Department of Biological Engineering, Massachusetts Institute of Technology, Cambridge, MA 02139; [b]Department of Biological Sciences, University at Albany, State University of New York, Albany, NY 12222; and [c]Center for Environmental Health Sciences, Massachusetts Institute of Technology, Cambridge, MA 02139

Deamination of nucleobases in DNA and RNA results in the formation of xanthine (X), hypoxanthine (I), oxanine, and uracil, all of which are miscoding and mutagenic in DNA and can interfere with RNA editing and function. Among many forms of nucleic acid damage, deamination arises from several unrelated mechanisms, including hydrolysis, nitrosative chemistry, and deaminase enzymes. Here we present a fourth mechanism contributing to the burden of nucleobase deamination: incorporation of hypoxanthine and xanthine into DNA and RNA caused by defects in purine nucleotide metabolism. Using *Escherichia coli* and *Saccharomyces cerevisiae* with defined mutations in purine metabolism in conjunction with analytical methods for quantifying deaminated nucleobases in DNA and RNA, we observed large increases (up to 600-fold) in hypoxanthine in both DNA and RNA in cells unable to convert IMP to XMP or AMP (IMP dehydrogenase, *guaB*; adenylosuccinate synthetase, *purA*, and *ADE12*), and unable to remove dITP/ITP and dXTP/XTP from the nucleotide pool (dITP/XTP pyrophosphohydrolase, *rdgB* and *HAM1*). Conversely, modest changes in xanthine levels were observed in RNA (but not DNA) from *E. coli* lacking *purA* and *rdgB* and the enzyme converting XMP to GMP (GMP synthetase, *guaA*). These observations suggest that disturbances in purine metabolism caused by known genetic polymorphisms could increase the burden of mutagenic deaminated nucleobases in DNA and interfere with gene expression and RNA function, a situation possibly exacerbated by the nitrosative stress of concurrent inflammation. The results also suggest a mechanistic basis for the pathophysiology of human inborn errors of purine nucleotide metabolism.

DNA and RNA damage | mass spectrometry | nucleobase deamination | purine metabolism | DNA repair

The chemical modification of nucleobases in DNA and RNA can arise from both physiological and adventitious mechanisms at all stages of nucleic acid metabolism. This is particularly true for deaminated versions of the nucleobases. As shown in Fig. 1 for purines, nucleobase deamination in DNA and RNA leads to the formation of 2′-deoxy- and ribonucleoside forms of hypoxanthine (2′-deoxyinosine, dI; inosine, Ino) from adenine, xanthine (2′-deoxyxanthosine, dX; xanthosine, Xao) and oxanine (2′-deoxyoxanosine, dO; oxanosine, Oxo) from guanine, and uracil (2′-deoxyuridine, dU; uridine, Urd) from cytosine (1). All of these products are miscoding and mutagenic in DNA (2–4) and can interfere with RNA editing (5) and the function of noncoding RNAs (6).

There are three recognized mechanisms that contribute to nucleobase deamination in DNA and RNA, the simplest of which is hydrolysis (7). A second source of nucleobase deamination is associated with the nitrosative stress caused by increases in nitric oxide-derived nitrous anhydride during inflammation (1). A third mechanism is associated with deaminase enzymes acting on RNA

and DNA, with activation-induced cytidine deaminase converting cytidine to uridine during immunoglobulin diversification in B lymphocytes and adenosine deaminases responsible for mRNA editing (5) and modification of tRNA and rRNA (8). Here we propose a fourth mechanism in which perturbation of purine nucleotide metabolism leads to incorporation of the purine intermediates hypoxanthine and xanthine into DNA and RNA.

Purine nucleotide metabolism plays a central role in cell physiology of both prokaryotes and eukaryotes (e.g., ref. 9). While purine biosynthesis contributes to many facets of cell metabolism, the present work focuses on synthesis of the purine nucleotide components of RNA and DNA, which is highly conserved in all organisms (10). As shown in Fig. 2 for *Escherichia coli*, purine anabolism is composed of a 10-step reaction starting with phosphoribosylpyrophosphate (PRPP) and ending with inosine monophosphate (IMP). Conversion of IMP to AMP is mediated by adenylosuccinate synthetase (*purA*) and followed by adenylosuccinate lyase (*purB*). GMP is also derived from IMP but via xanthosine monophosphate (XMP) through the action of IMP dehydrogenase (*guaB*) and GMP synthetase (*guaA*). Xanthine and hypoxanthine thus play significant roles in purine metabolism as components of the cellular nucleotide pool.

The concentrations of purine nucleotide pool components are highly regulated (11, 12), with many human diseases caused by imbalances arising from genetic polymorphisms and mutations in purine metabolism (13–17). For example, loss of adenosine deaminase results in severe combined immunodeficiency (18), while loss of hypoxanthine-guanine phosphoribosyltransferase leads to the hyperuricemia and neurological symptoms of Lesch–Nyhan syndrome (14), and increases in the activity of purine nucleotide metabolic enzymes, such as IMP dehydrogenase, are associated with several types of cancer (19). Further, genetic polymorphisms in purine metabolic enzymes are associated with the toxic side effects of thiopurine drugs (17). One possible mechanism underlying these pathologies and diseases involves the forma-
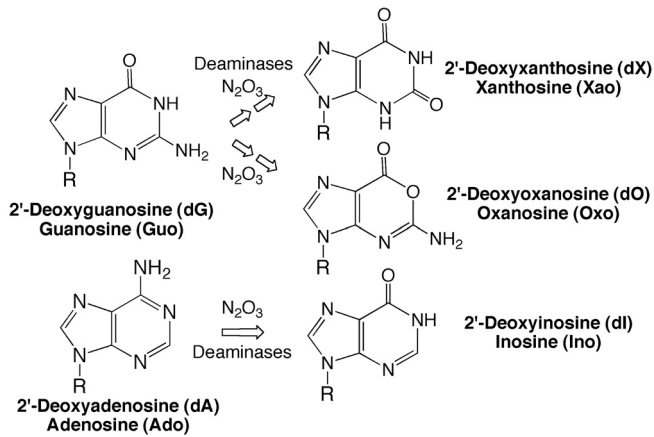
BIOCHEMISTRY

Fig. 1. Nucleobase deamination in DNA and RNA.

tion of noncanonical nucleotide triphosphosphates from nucleotide pool components, with subsequent incorporation into DNA and RNA. From the standpoint of mutagenesis, this would parallel the polymerase-induced misincorporation of canonical 2′-deoxyribonucleotides into DNA (e.g., ref. 20). Similar polymerase-induced misincorporation has been shown to occur with ribonucleotides during DNA synthesis (21), which leads to a potential mechanism for insertion of ribonucleotide forms of xanthine and hypoxanthine into DNA as well as RNA.

Given the potential for the nucleotide pool to affect genomic integrity, cells possess mechanisms to prevent incorporation of damaged nucleoside triphosphates into nucleic acids and to remove noncanonical nucleotides from DNA. For example, ribonucleotide insertions into DNA are repaired by a combination of RNase H and topoisomerase I in eukaryotic cells (22), while

Fig. 2. Purine nucleotide metabolism in *E. coli* and *S. cerevisiae*. Gene names: *E. coli*, green font; *S. cerevisiae*, blue font. Abbreviations: SAMP, adenylosuccinate; EndoV, endonuclease V; EndoVIII, endonuclease VIII; NDP kinase, nucleoside diphosphate kinase.

removal of xanthine and hypoxanthine from DNA is accomplished in *E. coli* by repair enzymes such as endonuclease V (EndoV; *nfi*), endonuclease VIII (EndoVIII; *nei*), alkyladenine glycosylase A (AlkA; *alkA*), and mismatch-specific uracil DNA glycosylase (MUG; *mug*) (23–26). Misinsertion of damaged nucleotides is partially controlled by polymerase substrate specificity, but a variety of enzymes have evolved to remove noncanonical nucleoside triphosphates from the nucleotide pool. *E. coli* possesses two nucleoside-triphosphatases, YjjX and RdgB, that cleave (d)XTP and (d)ITP to diphosphate (YjjX) and monophosphate (RdgB) forms (27–29), which parallels *E. coli* MutT pyrophosphorylase activity that acts on 8-oxo-dGTP (30). RdgB homologs in *S. cerevisiae*, mice, and humans (*ITPA*) possess similar activities (29, 31). Indeed, loss of ITPA in mice, though perinatal lethal, leads to increased incorporation of hypoxanthine in DNA and RNA (32, 33), which is alleviated by expression of the IDP-hydrolyzing activity of nudix-type motif 16 protein (NUDT16) (34).

The hypothesis tested here is that, beyond the enzymes that cleanse the nucleotide pool, defects in the biosynthetic network of purine metabolic enzymes lead to increased incorporation of xanthine and hypoxanthine into DNA and RNA. To test this model, we used chromatography-coupled isotope-dilution tandem mass spectrometry to quantify misincorporation of the deaminated nucleobases into the DNA and RNA of *E. coli* and *S. cerevisiae* strains possessing mutations in purine nucleotide metabolism. The results reveal that disruption of critical nodes in the purine metabolism network causes large increases of hypoxanthine, but not xanthine, in DNA and RNA. These results have implications for the pathophysiological mechanisms underlying many human metabolic disorders and suggest that disturbances in purine metabolism caused by known genetic polymorphisms could increase the burden of mutagenic deaminated nucleobases in DNA and interfere with gene expression and RNA function, a situation possibly exacerbated by the nitrosative stress of concurrent inflammation.

Results

Quantification of Deaminated Nucleotides in DNA and RNA. To complement our method for quantifying dX, dI, dO, and dU (Fig. 1) (35), we developed an isotope-dilution LC-MS/MS method for quantifying their ribonucleoside equivalents. This involves hydrolysis of RNA, HPLC purification of ribonucleosides ([Fig. S1](#)), and their quantification by LC-MS/MS using predetermined molecular transitions. While quantitative rigor is ensured with istopically labeled internal standards, DNA and RNA deamination artifacts were minimized with deaminase inhibitors (35).

The results of analysis of xanthine and hypoxanthine in RNA and DNA in *E. coli* strains are shown in Table 1 and those for *S. cerevisiae* in Table 2. In all studies, the *G* deamination products dO and Oxo were below detection limits (<5 oxanine per 10^8 nt), which is consistent with previous studies in human cells and mouse tissues (36, 37). It was also apparent that the levels of xanthine and hypoxanthine were higher in wild-type *E. coli* RNA than in DNA, by twofold and ninefold, respectively. This is not surprising because Ino is one of many ribonucleoside modifications in tRNA and rRNA (8). As a negative control for these studies, we observed that the level of dU in wild-type and mutant *E. coli* strains was constant at approximately 5 per 10^5 nt, which is consistent with mutations that do not involve pyrimidine metabolism.

Defects in Purine Nucleotide Metabolism Increase the Levels of Xanthine and Hypoxanthine in RNA and DNA. Focusing first on data for hypoxanthine in *E. coli* (Table 1), it is apparent that the loss of individual *E. coli* genes leads to substantial increases in the levels of dI and Ino. Loss of either enzyme that acts on IMP to initiate formation of guanine nucleotides (*guaB*) or adenine nucleotides (*purA*) causes twofold to sevenfold increases in Ino and smaller
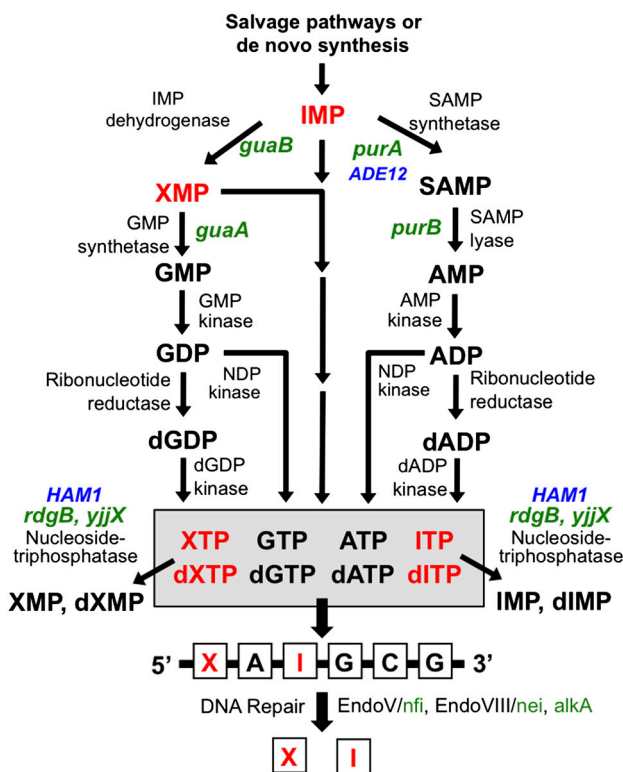
Table 1. Levels of Ino, Xao, dI, and dX in genomic DNA and total RNA from *E. coli* lacking purine nucleotide metabolism genes*

Genotype	Ino	Xao	dI	dX
Wild type	11 ± 3	2.8 ± 0.5	1.2 ± 0.2	1.3 ± 0.3
purA	25 ± 4[†]	3.0 ± 0.8	1.5 ± 0.4	1.1 ± 0.3
guaB	74 ± 14[†]	1.5 ± 0.3[†]	4.2 ± 0.7[†]	2.2 ± 1.1
rdgB	100 ± 20[†]	3.3 ± 0.6	5.8 ± 0.5[†]	1.2 ± 0.2
yjjX	13 ± 3	3.1 ± 0.4	1.1 ± 0.2	1.1 ± 0.2
nfi	11 ± 1	2.6 ± 0.2	0.8 ± 0.2	1.4 ± 0.3
purA/guaB	39 ± 24	1.2 ± 0.03[†]	3.1 ± 0.09[†]	1.2 ± 0.4
purA/nfi	30 ± 5[†]	3.6 ± 0.8	0.9 ± 0.1	1.4 ± 0.4
purA/rdgB	2,100 ± 200[†]	2.8 ± 0.7	280 ± 80[†]	1.6 ± 0.1
guaB/rdgB	813 ± 125[†]	1.5 ± 0.09[†]	100 ± 7[†]	1.2 ± 0.4
rdgB/yjjX	80 ± 20[†]	3.3 ± 0.4	5.8 ± 0.5[†]	1.4 ± 0.2
rdgB/nfi	100 ± 20[†]	3.5 ± 0.7	6.0 ± 0.5[†]	1.0 ± 0.1
purA/guaA/rdgB	1,700 ± 300[†]	7.2 ± 0.5[†]	200 ± 10[†]	1.8 ± 0.4
purA/guaB/rdgB	2,900 ± 400[†]	2.1 ± 2.1	770 ± 200[†]	1.2 ± 0.2
purA/guaB/yjjX	30 ± 7[†]	1.1 ± .05[†]	4.0 ± 1.6[†]	2.0 ± 1.9
purA/guaB/nfi	2,100 ± 200[†]	2.2 ± 0.6	220 ± 50[†]	1.9 ± 0.5
purA/guaA/rdgB/nfi	1,900 ± 400[†]	6.5 ± 0.3[†]	250 ± 30[†]	1.7 ± 0.2
purA/guaB/rdgB/nfi	2,400 ± 400[†]	3.3 ± 0.4	620 ± 180[†]	1.6 ± 0.3
purA/guaB/rdgB/ alkA	1,971 ± 212[†]	1.2 ± 0.06[†]	689 ± 112[†]	1.5 ± 0.4

*Data represent mean ± SD for n = 3; units of lesions per 10^6 nt.
[†]Significantly different from wild type at $P < 0.05$ by Student's *t* test.

increases in dI. This is consistent with reduced consumption of IMP leading to formation of ITP and dITP by aberrant kinase and ribonucleotide reductase activity. However, this argument would suggest that loss of both IMP dehydrogenase (*guaB*) and adenylosuccinate synthetase (*purA*) would lead to higher levels of dI and Ino, but this is not the case (Table 1). Further, these increases are not prevented by the (d)ITP-hydrolyzing RdgB, which suggests that generation of (d)ITP exceeds the enzymatic capacity of the pool cleansing enzymes.

Not surprisingly, loss of the RdgB nucleoside triphosphatase led to a 10-fold and fivefold increase in Ino and dI, respectively, which is consistent with its role in removing deaminated nucleoside triphosphates from the pool. However, loss of the similar YjjX nucleoside triphosphatase, even in combination with loss of RdgB, had no effect on xanthine or hypoxanthine levels (Table 1). Both enzymes have in vitro activities against (d)XTP and (d)ITP (27–29), so the results suggest that RdgB is the major xanthine and hypoxanthine nucleoside triphosphatase in *E. coli* and that the in vivo substrate specificities need to be reconsidered. Finally, the loss of either the *nfi* gene encoding the EndoV DNA repair protein or the *alkA* gene encoding the AlkA DNA glycosylase did not affect the levels of xanthine or hypoxanthine in DNA or RNA; the implications of this observation will be discussed shortly in the context of DNA repair.

While the loss of single genes in purine metabolism led to substantial changes in hypoxanthine levels, losses of specific combinations of genes led to synergistic increases in the content of hypoxanthine in DNA and RNA. The most striking effect occurred with loss of both *rdgB* and *purA* genes, which led to large increases in dI and Ino ranging from 155- to 642-fold. This can be rationalized as a loss of PurA causing an increase in IMP concentration that then results in increased levels of dITP and ITP in the nucleotide pools, with the absence of RdgB allowing incorporation of dITP and ITP by polymerases into DNA and RNA. This model is supported by the fact that the largest changes in dI and Ino occur with loss of both *purA* and *guaB* along with *rdgB* (Table 1).

The data in Table 1 also reveal important information about mechanisms of DNA repair. While EndoV has activity against dI, dX and dO (25) and AlkA has activity against dI (23–25, 38), the loss of either enzyme did not result in elevated levels of dI (Table 1). There may thus be a redundancy in the repair capacity for dI, with EndoVIII (*nei*) also showing in vitro activity with dI (23–25). It is worth noting that the *purA/rdgB* and *guaB/rdgB* double mutants maintain high levels of dI in spite of the activity of dI repair enzymes. This raises questions about the mechanisms controlling steady-state levels of DNA damage.

Finally, a review of the data in Table 1 reveals that the mutations caused few significant changes in the levels of dX and Xao. For example, the only statistically significant increase in Xao occurred in the *purA/rdgB/guaA* triple mutant, which is consistent with increases in XMP caused by failure to convert it to GMP by GMP synthetase (*guaA*). However, the magnitude of the increase in Xao (approximately threefold) is considerably smaller than the analogous change observed in Ino with loss of *purA* and *rdgB* (Table 1).

The studies for hypoxanthine levels in *S. cerevisiae* yielded similar results as those in *E. coli*. As shown in Table 2, loss of either *ADE12*, the equivalent of *E. coli purA*, or *HAM1*, an *rdgB* ortholog, did not affect dI or Ino levels. However, loss of both enzymes led to 36- and 49-fold increases in hypoxanthine in RNA and DNA, respectively.

Discussion

Our results reveal that defects in purine metabolism represent a mechanism for the pathological incorporation of deaminated nucleotides into DNA and RNA. These studies reveal nodes in the purine metabolic network that, when disrupted, have significant consequences for genetic toxicology and RNA function. Given the conservation of purine metabolism, the discovery of similar nodes in both *E. coli* and yeast should have relevance to the strong association in humans between purine metabolic defects and pathology and disease. As shown in Fig. 2, the genes with the greatest effect on hypoxanthine incorporation into DNA and RNA are located early (*purA, guaB*) in the metabolic pathways or later at the "pool cleansing" step prior to incorporation of nucleotides into nucleic acids (*rdgB*). The latter is consistent with the observation that loss of the mammalian *rdgB* homolog, *ITPA*, leads to increases in ITP in the nucleotide pool and incorporation of hypoxanthine into DNA and RNA in a knockout mouse model (32–34). That loss of *purA* or *guaB* would cause twofold to 10-fold increases of hypoxanthine in DNA and RNA is reasonable given the accumulation of IMP that could be presumed to occur with loss of the enzymes, with excess IMP becoming a substrate for kinases and ribonucleotide reductases in the metabolic network (Fig. 2). These critical metabolic steps are also subject to genetic polymorphisms in humans, with significant implications for misincorporation of hypoxanthine in DNA and RNA. For example, a *T*-to-*G* substitution in the promoter region of the human *IMPDH2* gene, a homolog of *E. coli purA* encoding SAMP synthetase (Fig. 1), reduced gene expression by 50–60% (15). While the present studies focused on a complete loss of this gene, it is reasonable to assume that a 50–60% decrease in SAMP synthetase activity could cause measurable increases in hypoxanthine incorporation into DNA and RNA in human cells affected with the genetic polymorphism. That a 50% decrease in the activity of a purine nucleotide-related enzyme could cause increased incorporation of toxic nucleotides into DNA and RNA is supported by recent studies of genetic polymorphisms in the

Table 2. Levels of Ino and dI in genomic DNA and total RNA from *S. cerevisiae* lacking purine nucleotide metabolism genes*

Genotype	Ino per 10^6 nt	dI per 10^6 nt
Wild type	42 ± 8	2.0 ± 0.1
ade12	35 ± 5	3.0 ± 0.6
ham1	40 ± 10	2.2 ± 0.2
ade12/ham1	1,500 ± 72[†]	98 ± 20[†]

*Data represent mean ± SD for n = 3.
[†]Significantly different from wild type at $P < 0.05$ by Student's *t* test.

human *rdgB* homolog, *ITPA*. A common polymorphism in *ITPA*, the 94C > A allele present in 11–19% of Asians, reduces enzyme activity by 50% (16) and is associated with toxic responses to thiopurine therapy for cancer, autoimmune disease and inflammatory bowel disease (17), presumably due to increased incorporation of thiopurines into DNA and RNA. This parallels the fivefold and 10-fold increases in hypoxanthine in DNA and RNA, respectively, caused by loss of *rdgB* in *E. coli*.

Compared to the loss of *purA*, *guaB* or *rdgB* as individual genes, disruption of a combination of early and late enzymes produced synergistic increases in hypoxanthine incorporation into DNA and RNA (Table 1). Specifically, combined loss of *rdgB* and either *purA* or *guaB*, which individually produced twofold to ninefold increases in hypoxanthine in RNA, caused 80- to 190-fold increases (Table 1). A similar synergy was observed in yeast with loss of *ADE12* and *HAM1* (Table 2). These synergies suggest that even modest changes in the activities of pairs of these enzymes caused by genetic polymorphisms could result in increased misincorporation of hypoxanthine into nucleic acids in humans. Given the large reductions in activity caused by common genetic polymorphisms in the human homologs of *purA* and *rdgB* (15, 16), a substantial number of humans could possess polymorphisms that affect two or more purine metabolism genes, with the consequence of increased incorporation of deaminated nucleotides into DNA and RNA.

An intriguing feature of these studies was the lack of effect of metabolic defects on nucleic acid levels of xanthine, which could be due to any of several possible mechanisms. For DNA, it is possible that dI and dX are repaired with different efficiencies by the various activities of EndoV, EndoVIII, AlkA, and MUG (23–26). However, while DNA repair efficiency could account for some portion of the differing levels of xanthine and hypoxanthine in DNA, their differing levels in RNA suggest other mechanisms. Three examples support a model in which xanthine- and hypoxanthine-containing nucleotides interact differently with purine metabolic enzymes. First, xanthine nucleotides may bind less effectively in allosteric feedback mechanisms that are known to be important for regulation of ribonucleotide reductases (39). As another example, since the *purA/guaA/rdgB* mutation should cause reduced levels of ATP and GTP, reductions in ATP-dependent NAD^+ synthesis could lead to decreased activity of the NAD^+-dependent IMP dehydrogenase (*guaB*), which would reduce XMP synthesis. A third possibility is that xanthine-containing nucleotides are poorer substrates for kinases than hypoxanthine species. Agarwal et al. showed that GMP, dGMP, 8-azaGMP, and IMP are substrates for human guanylate kinase while XMP, UMP, CMP, and 6-thioIMP are not (40, 41). Thus, lower levels of (d)XTP may be due to less efficient phosphorylation of XMP.

Two other mechanisms may account for reduced xanthine incorporation into nucleic acids in the event that the levels of nucleoside triphosphates are equivalent. First, it is possible that (d)XTP are poorer substrates than (d)ITP for RNA and DNA polymerases, respectively, which is supported by the known selectivity of several polymerases (42, 43). Second, there may be a cryptic xanthine nucleoside triphosphatase beyond RdgB and YjjX. These alternatives await quantification of the components of the nucleoside triphosphate pool.

The phenomenon of purine metabolic defects leading to incorporation of deaminated nucleobases into nucleic acids should have pathological consequences in a variety of cellular processes. With respect to mutagenesis, while there is some controversy about the ability of hypoxanthine to induce mutations in *E. coli* (4, 44), dI, dX, and dU are all established mutagens in higher organisms. So it is reasonable to assume that genetic polymorphisms that raise the steady-state levels of dX and dI in DNA in humans would exacerbate the toxicity associated with the nitrosative stress of chronic inflammation, with further increases in dX

and dI exceeding the cell's repair capacity and contributing to mutations and cancer risk.

Considering both coding and noncoding RNA species, the incorporation of xanthine and hypoxanthine into RNA should have pathological consequences for gene expression. For example, editing of mRNA by ADAR-mediated conversion of adenine to hypoxanthine is a highly regulated mechanism controlling gene expression (5). The insertion of Ino into mRNA could thus be interpreted as inappropriate editing, with consequential sequestration of the mal-edited mRNA into heterochromatin (45) or entry into RNAi pathways (5). Given the role of Ino as an abundant posttranscriptional modification of RNA, misinsertion of Ino into tRNA and rRNA could affect translational fidelity and efficiency, as supported by recent observations (e.g., refs. 46 and 47).

Finally, increased concentrations of (d)XTP and (d)ITP could lead to enhanced incorporation of ribonucleotides into DNA and 2′-deoxyribonucleotides into RNA. The former has been observed with canonical ribonucleotides as a result of polymerase infidelity and leads to genomic instability if the levels of incorporated ribonucleotides exceed the capacity of RNase H and other repair enzymes to correct the insertion errors (21, 48). The combined effect of incorrect nucleotide class and noncanonical nucleobase caused by insertion of ITP or XTP into DNA could further complicate the pathophysiology of the polymerase errors.

Our observations suggest that disturbances in purine metabolism could increase the burden of mutagenic deaminated nucleobases in DNA and interfere with gene expression and RNA function, a situation possibly exacerbated by the nitrosative stress of concurrent inflammation. The results also suggest a mechanistic basis for the pathophysiology of human inborn errors of purine nucleotide metabolism.

Materials and Methods

Materials and Instruments. Chemicals and reagents were used without further purification unless otherwise noted and were obtained as follows: Nuclease P1: USBiological and Roche Diagnostic; coformycin: National Cancer Institute; uniformly ^{15}N-labeled Ado, Guo, dA, dG and dC: Cambridge Isotope Laboratories (Andover, MA); phosphodiesterase I: USB; alkaline phosphatase, desferroxamine, RNase A, ammonium acetate, tetrahydrouridine, DNase I: Sigma Chemical; UV-grade acetonitrile: Honeywell Burdick & Jackson; Milli-Q system for all water purification and Microcon YM-10 filters: Millipore; Genomic-tip 100/*G* kits, RNeasy Mini kits and RNAlater reagent: Qiagen (Valencia, CA). Instruments used: Agilent Bioanalyzer series 2100, Agilent 1100 HPLC system (LC), Agilent LC/QQQ 6460 triple quadrupole mass spectretometer (MS/MS), Applied Biosystems API 3000 MS/MS and Agilent LC/QTOF 6520 quadrupole time-of-flight mass spectrometer (QTOF).

Synthesis of Isotopically Labeled Internal Standards. Syntheses of [^{15}N$_4$]-labeled dX, dI and dO are described elsewhere (35). Xao, Ino, Oxo were synthesized similarly starting with uniformly ^{15}N-labeled Ado and Guo. All standards were purified by HPLC with a Phenomenex LUNA C18 column (250 mm × 4.6 mm, 5 μm, 100 Å pore), characterized by QTOF mass spectrometry, and quantified by UV absorbance (35, 49).

Preparation of *E. coli* and *S. cerevisiae* Mutants. *E. coli* mutants were constructed in a W3110 background by transduction using bacteriophage P1 vir. Individual mutant genes were obtained from the Keio Collection (50), as gene knockouts carrying a kanamycin gene cartridge, and were transduced into *E. coli* W3110 using selection for kanamycin resistance, with the resistance cartridge removed using flp sequences surrounding the kanamycin cartridge and flp recombinase (51). Additional rounds of transduction and gene cartridge removal yielded the multiple mutant strains. The phenotypes of *purA* mutants and *guaA* and *guaB* mutants were confirmed by an inability to grow in the absence of Ade and Gua, respectively. The *alkA* mutant phenotype was confirmed by sensitivity to methylmethane sulfonate and genotypes of *rdgB*, *yggX*, and *nfi* mutants were confirmed by PCR.

The *S. cerevisiae* strains are from the Saccharomyces Genome Deletion Project (52). To construct the *ham1::URA3 ade12::KANMX4* double mutant strain, a two-step cloning process was performed. In the first step, a *ham1::KANMX4* DNA sequence was amplified from *S. cerevisiae ham1* mutant genomic DNA using the 5′primer GGCCGCGGAATTCCTTTTCAAGCATGAAATCGCC-

TA and the 3′ primer GGCCGCGGAATTCGACATTTCGGCAGGTGACTTCAG. PCR amplified products were digested with EcoR1 and ligated into EcoR1-cleaved pUC19. The two internal ClaI restriction sites in the KANMX4 gene were utilized to construct the second clone, for which the *URA3* gene was amplified from CYP225 *tmpl1* URA3 genomic DNA using the 5′ primer CTGCGCCAATC-GATGACAATACAGACGATG, and the 3′ primer GTCTGTGAAACATCGATCTAC-CAGATTAGAGTACA. PCR products were digested with ClaI and ligated into ClaI-cleaved *ham1::KANMX4* pUC19 vector, with the *ham1::URA3* DNA sequence subsequently amplified using the same primers for the *ham1::KANMX4* sequence in step one. To obtain the *ham1::URA3 ade12::KANMX4* double mutant, the amplified sequence was transformed into a *S. cerevisiae ade12::KANMX4* mutant strain (Geitz Lab Yeast Transformation Kit Quick and Easy protocol). Plating on yeast nitrogen base agar plates lacking uracil was used to select for *ham1::URA3 ade12::KANMX4* transformants. The phenotype of *ade12* mutants was confirmed by their inability to grow in the absence of Ade and that of *ham1* mutants by their sensitivity to 6-hydroxylaminopurine.

DNA and RNA Purification. Following collection of bacterial and yeast, genomic DNA was purified (Genomic-tip 100/*G* kit) in the presence of deaminase inhibitors coformycin (5 μg/mL) and tetrahydrouridine (125 μg/mL) to avoid nucleobase deamination artifacts (35). Total RNA was isolated from bacteria (QiagenRNeasy Mini Kit) with coformycin and tetrahydrouridine. DNA and RNA were initially quantified by UV absorbance for preparation of hydrolysates and subsequently, for normalization of mass spectrometry data, by quantification of canonical nucleosides during HPLC resolution using external calibration curves.

DNA and RNA Hydrolysis. Total RNA or genomic DNA (50 μg) was lyophilized and redissolved in 30 μL of ammonium acetate buffer (30 mM, pH 6.2) to which zinc chloride (10 μL, 10 mM) and [^{15}N]-labeled internal standards (10 pmol) were added to yield a final volume of 50 μL. DNA was hydrolyzed by addition of nuclease P1 (4 U) and DNaseI (5 U) with incubation at 37 °C for 3 h, followed by dephosphorylation by addition of ammonium acetate buffer (30 mM, pH 7.4), coformycin (5 μg/mL), tetrahydrouridine (125 μg/mL), alkaline phosphatase (15 U) and phosphodiesterase I (1.0 U) and incubation at 37 °C for 6 h. The enzymes were subsequently removed by Microcon YM-10 filtration. Total RNA was processed similarly, with the exception of initial hydrolysis in 30 mM ammonium acetate and 2 mM ZnCl$_2$ (pH 6.8) with nuclease P1 (1 U) and RNase A (5 U) for 3 h at 37 °C and dephosphorylation with alkaline phosphatase (10 U) and phosphodiesterase I (0.5 U) for 1 h at 37 °C following addition of acetate buffer to 30 mM, pH 7.8.

Prepurification of X- and I-Containing Nucleosides. dI, dX, dO, and dU in DNA were resolved by reversed-phase HPLC as noted earlier at a flow rate of 0.4 mL/min with a stepwise acetonitrile gradient in 4 mM ammonium acetate (pH 7.4): 0–40 min, 1–8% acetonitrile; 40–45 min, 8–50%; 45–50 min, 50%; 50–51 min, 50–1% (reversal); 51–61 min, 1%. Individual nucleosides were collected at predefined retention times: dX, 19 min; dU, 27 min; dI,

34 min; and dO, 45 min; for canonical nucleosides: dC, 22 min, dG, 36 min, T, 39.5 min, and dA, 50.5 min. Ino and Xao in RNA hydrolysates were also purified by HPLC using the same Phenomenex Synergi C18 column (250 × 4.6 mm, 4 μm particle, 80 Å pore), with a flow rate of 0.5 mL/min and acetonitrile gradient in 8 mM ammonium acetate (pH 6.9) at 36 °C: 0–18 min, 1–2%; 18–23 min, 2%; 23–28 min, 2–7%; 28–30 min, 7%; 30–31 min, 7–100%; 31–41 min, 100%. Individual nucleosides were collected at experimentally determined retention times (min): Xao, 22; Ino, 31; Oxo, 40; canonical nucleosides eluted as follows (min): Cyd, 16; Urd, 17.5; Guo, 32; Ado, 46.5. For both DNA and RNA, fractions containing individual nucleosides were dried under vacuum and redissolved in 45 μL of water for analysis by LC-MS/MS.

Quantification of X- and I-Containing Nucleosides. Individual 2′-deoxyribonucleosides were quantified using an Agilent 1100 HPLC system coupled to an API 3000 MS/MS. Reversed-phased HPLC separation was carried out using a Thermo Hypersil GOLD aQ column (150 × 2.1 mm, 3 μm particle). A 20 μL injection volume was eluted isocratically at a flow rate of 100 μL/min with a mobile phase consisting of 0.1% acetic acid and acetonitrile at volume ratio of 97:3. The mass spectrometer was operated with a turbo ionspray source at 380 °C in positive ion mode, with unit resolution for Q1 and Q3, and other optimized parameters: ion source voltage, 4.0 kV; nebulizer gas, 8; curtain gas, 8; collision gas (N_2), 4; declustering potential, 20; focusing potential, 100; entrance potential, 5; collision energy, 10; collision cell exit potential, 10. MRM was used for detection of nucleosides with a dwell time to 200 ms. Q1 was set to transmit the precursor ions MH+ at m/z 273, 257, and 231 for the internal standards [^{15}N$_4$]-dX/dO, dI, and dU, respectively; at m/z 269, 253, and 229 for dX/dO, dI, and dU, respectively. The product ions were monitored in Q3 at m/z 157, 141, and 115 for internal standards [^{15}N$_4$]-X/O, I, and U; at m/z 153, 137, and 111 for X/O, I, and U, respectively. Linear calibration curves were obtained daily.

Ribonucleosides were injected onto the same HPLC column eluted isocratically at 200 μL/min with an aqueous mobile phase consisting of 0.1% acetic acid and 1% acetonitrile. The eluent was analyzed by Agilent MS/MS operated with an electrospray ion source at 350 °C and in positive ion mode, with wide resolution for Q1 and unit resolution for Q3, and other optimized parameters: capillary voltage, 4.0 kV; nebulizer gas, 20 psi; collision gas (N_2), 10 L min^{-1}; fragmentor potential, 65 V; collision energy, 6; delta EMV, 700 V. MRM was used for detection of nucleosides, with Q1 set to transmit the precursor ions MH+ at m/z 289 and 269 for internal standards [^{15}N$_4$]-Xao/Oxo and Ino, respectively; at m/z 285 and 273 for Xao/Oxo and Ino. The product ions were monitored in Q3 at m/z 157 and 141 for internal standards [^{15}N$_4$]-X/O and I; at m/z 153 and 137 for X/O and I, respectively. The limits of detection for Ino, Xao, and Oxo were 5, 10, and 50 fmol, respectively.

1. Dedon PC, Tannenbaum SR (2004) Reactive nitrogen species in the chemical biology of inflammation. *Arch Biochem Biophys* 423:12–22.
2. Yasui M, et al. (2008) Miscoding properties of 2′-deoxyinosine, a nitric oxide-derived DNA Adduct, during translesion synthesis catalyzed by human DNA polymerases. *J Mol Biol* 377:1015–1023.
3. Wuenschell GE, O'Connor TR, Termini J (2003) Stability, miscoding potential, and repair of 2′-deoxyxanthosine in DNA: implications for nitric oxide-induced mutagenesis. *Biochemistry* 42:3608–3616.
4. Hill-Perkins M, Jones MD, Karran P (1986) Site-specific mutagenesis in vivo by single methylated or deaminated purine bases. *Mutat Res* 162:153–163.
5. Bass BL (2002) RNA editing by adenosine deaminases that act on RNA. *Annu Rev Biochem* 71:817–846.
6. Agris PF, Vendeix FA, Graham WD (2007) tRNA's wobble decoding of the genome: 40 years of modification. *J Mol Biol* 366:1–13.
7. Shen JC, Rideout WM, 3rd, Jones PA (1994) The rate of hydrolytic deamination of 5-methylcytosine in double-stranded DNA. *Nucleic Acids Res* 22:972–976.
8. Söll D, RajBhandary U (1995) *tRNA: Structure, Biosynthesis and Function* (ASM Press, Washington, DC).
9. Mathews CK, Van Holde KE, Ahern KG, eds. (1999) *Biochemistry* (Prentice Hall, New York), 3 Ed.
10. Kappock TJ, Ealick SE, Stubbe J (2000) Modular evolution of the purine biosynthetic pathway. *Curr Opin Chem Biol* 4:567–572.
11. Bennett BD, et al. (2009) Absolute metabolite concentrations and implied enzyme active site occupancy in *Escherichia coli*. *Nat Chem Biol* 5:593–599.
12. Mathews CK (2006) DNA precursor metabolism and genomic stability. *FASEB J* 20:1300–1314.
13. Stepchenkova EI, et al. (2009) Functional study of the P32T ITPA variant associated with drug sensitivity in humans. *J Mol Biol* 392:602–613.
14. Stanbury JB (1983) *The Metabolic Basis of Inherited Disease* (McGraw-Hill, NY), 5th Ed,, pp xvi–2032.
15. Garat A, et al. (2009) IMPDH2 genetic polymorphism: A promoter single-nucleotide polymorphism disrupts a cyclic adenosine monophosphate responsive element. *Genet Test Mol Biomarkers* 13:841–847.
16. Herting G, Barber K, Zappala MR, Cunningham RP, Burgis NE (2010) Quantitative in vitro and in vivo characterization of the human P32T mutant ITPase. *Biochim Biophys Acta* 1802:269–274.
17. Stocco G, Crews KR, Evans WE (2010) Genetic polymorphism of inosine-triphosphate-pyrophosphatase influences mercaptopurine metabolism and toxicity during treatment of acute lymphoblastic leukemia individualized for thiopurine-S-methyl-transferase status. *Expert Opin Drug Saf* 9:23–37.
18. Buckley RH (2004) Molecular defects in human severe combined immunodeficiency and approaches to immune reconstitution. *Annu Rev Immunol* 22:625–655.
19. Hodges SD, Fung E, McKay DJ, Renaux BS, Snyder FF (1989) Increased activity, amount, and altered kinetic properties of IMP dehydrogenase from mycophenolic acid-resistant neuroblastoma cells. *J Biol Chem* 264:18137–18141.
20. Kunz BA, et al. (1994) International Commission for Protection Against Environmental Mutagens and Carcinogens Deoxyribonucleoside triphosphate levels: A critical factor in the maintenance of genetic stability. *Mutat Res* 318:1–64.
21. Nick McElhinny SA, et al. (2010) Genome instability due to ribonucleotide incorporation into DNA. *Nat Chem Biol* 6:774–781.
22. Kim N, et al. (2011) Mutagenic processing of ribonucleotides in DNA by yeast topoisomerase I. *Science* 332:1561–1564.
23. Dong M, et al. (2006) Development of enzymatic probes of oxidative and nitrosative DNA damage caused by reactive nitrogen species. *Mutat Res* 594:120–134.

BIOCHEMISTRY

24. Terato H, et al. (2002) Novel repair activities of AlkA (3-methyladenine DNA glycosylase II) and endonuclease VIII for xanthine and oxanine, guanine lesions induced by nitric oxide and nitrous acid. *Nucleic Acids Res* 30:4975–4984.

25. Kow YW (2002) Repair of deaminated bases in DNA. *Free Radic Biol Med* 33:886–893.

26. Lee HW, Brice AR, Wright CB, Dominy BN, Cao W (2010) Identification of *Escherichia coli* mismatch-specific uracil DNA glycosylase as a robust xanthine DNA glycosylase. *J Biol Chem* 285:41483–41490.

27. Chung JH, Park HY, Lee JH, Jang Y (2002) Identification of the dITP- and XTP-hydrolyzing protein from *Escherichia coli. J Biochem Mol Biol* 35:403–408.

28. Burgis NE, Brucker JJ, Cunningham RP (2003) Repair system for noncanonical purines in *Escherichia coli. J Bacteriol* 185:3101–3110.

29. Burgis NE, Cunningham RP (2007) Substrate specificity of RdgB protein, a deoxyribonucleoside triphosphate pyrophosphohydrolase. *J Biol Chem* 282:3531–3538.

30. Nakabeppu Y, Oka S, Sheng Z, Tsuchimoto D, Sakumi K (2010) Programmed cell death triggered by nucleotide pool damage and its prevention by MutT homolog-1 (MTH1) with oxidized purine nucleoside triphosphatase. *Mutat Res* 703:51–58.

31. Lin S, et al. (2001) Cloning, expression, and characterization of a human inosine triphosphate pyrophosphatase encoded by the itpa gene. *J Biol Chem* 276:18695–18701.

32. Behmanesh M, et al. (2009) ITPase-deficient mice show growth retardation and die before weaning. *Cell Death Differ* 16:1315–1322.

33. Sakumi K, et al. (2010) ITPA protein, an enzyme that eliminates deaminated purine nucleoside triphosphates in cells. *Mutat Res* 703:43–50.

34. Abolhassani N, et al. (2010) NUDT16 and ITPA play a dual protective role in maintaining chromosome stability and cell growth by eliminating dIDP/IDP and dITP/ITP from nucleotide pools in mammals. *Nucleic Acids Res* 38:2891–2903.

35. Taghizadeh K, et al. (2008) Quantification of DNA damage products resulting from deamination, oxidation and reaction with products of lipid peroxidation by liquid chromatography isotope dilution tandem mass spectrometry. *Nat Protoc* 3:1287–1298.

36. Dong M, Dedon PC (2006) Relatively small increases in the steady-state levels of nucleobase deamination products in DNA from human TK6 cells exposed to toxic levels of nitric oxide. *Chem Res Toxicol* 19:50–57.

37. Pang B, et al. (2007) Lipid peroxidation dominates the chemistry of DNA adduct formation in a mouse model of inflammation. *Carcinogenesis* 28:1807–1813.

38. Feng H, Klutz AM, Cao W (2005) Active site plasticity of endonuclease V from *Salmonella typhimurium. Biochemistry* 44:675–683.

39. Reichard P (2010) Ribonucleotide reductases: Substrate specificity by allostery. *Biochem Biophys Res Commun* 396:19–23.

40. Agarwal RP, Scholar EM, Agarwal KC, Parks RE, Jr (1971) Identification and isolation on a large scale of guanylate kinase from human erythrocytes. Effects of monophosphate nucleotides of purine analogs. *Biochem Pharmacol* 20:1341–1354.

41. Agarwal KC, Miech RP, Parks RE, Jr (1978) Guanylate kinases from human erythrocytes, hog brain, and rat liver. *Methods Enzymol* 51:483–490.

42. Valentine MR, Termini J (2001) Kinetics of formation of hypoxanthine containing base pairs by HIV-RT: RNA template effects on the base substitution frequencies. *Nucleic Acids Res* 29:1191–1199.

43. Rogstad KN, Jang YH, Sowers LC, Goddard WA, 3rd (2003) First principles calculations of the pKa values and tautomers of isoguanine and xanthine. *Chem Res Toxicol* 16:1455–1462.

44. Budke B, Kuzminov A (2006) Hypoxanthine incorporation is nonmutagenic in *Escherichia coli. J Bacteriol* 188:6553–6560.

45. Fernandez HR, Kavi HH, Xie W, Birchler JA (2005) Heterochromatin: on the ADAR radar? *Curr Biol* 15:R132–134.

46. Chan CT, et al. (2010) A quantitative systems approach reveals dynamic control of tRNA modifications during cellular stress. *PLoS Genet* 6:e1001247.

47. Wohlgamuth-Benedum JM, et al. (2009) Thiolation controls cytoplasmic tRNA stability and acts as a negative determinant for tRNA editing in mitochondria. *J Biol Chem* 284:23947–23953.

48. Clark AB, Lujan SA, Kissling GE, Kunkel TA (2011) Mismatch repair-independent tandem repeat sequence instability resulting from ribonucleotide incorporation by DNA polymerase varepsilon. *DNA Repair* 10:476–482.

49. Yu H, Venkatarangan L, Wishnok JS, Tannenbaum SR (2005) Quantitation of four guanine oxidation products from reaction of DNA with varying doses of peroxynitrite. *Chem Res Toxicol* 18:1849–1857.

50. Baba T, et al. (2006) Construction of *Escherichia coli* K-12 in-frame, single-gene knockout mutants: The Keio collection. *Mol Syst Biol* 2:2006 0008.

51. Datsenko KA, Wanner BL (2000) One-step inactivation of chromosomal genes in *Escherichia coli* K-12 using PCR products. *Proc Natl Acad Sci USA* 97:6640–6645.

52. Winzeler EA, et al. (1999) Functional characterization of the S. cerevisiae genome by gene deletion and parallel analysis. *Science* 285:901–906.